Developmental Biology 432 (2017) 286–297

Contents lists available at ScienceDirect

Developmental Biology

journal homepage: www.elsevier.com/locate/developmentalbiology

Transcriptional regulation of *Nfix* by NFIB drives astrocytic maturation within the developing spinal cord

Elise Matuzelski[a], Jens Bunt[b], Danyon Harkins[a], Jonathan W.C. Lim[b], Richard M. Gronostajski[c], Linda J. Richards[a,b], Lachlan Harris[a,1], Michael Piper[a,b,*,1]

[a] School of Biomedical Sciences, The Faculty of Medicine, The University of Queensland, Brisbane 4072, Queensland, Australia
[b] Queensland Brain Institute, The University of Queensland, Brisbane 4072, Queensland, Australia
[c] Department of Biochemistry, Program in Genetics, Genomics and Bioinformatics, Center of Excellence in Bioinformatics and Life Sciences, State University of New York at Buffalo, Buffalo 14260, NY, USA

ARTICLE INFO

Keywords:
Nuclear Factor I
NFIX
NFIA
NFIB
Spinal cord
Gliogenesis
GFAP
Astrocyte

ABSTRACT

During mouse spinal cord development, ventricular zone progenitor cells transition from producing neurons to producing glia at approximately embryonic day 11.5, a process known as the gliogenic switch. The transcription factors Nuclear Factor I (NFI) A and B initiate this developmental transition, but the contribution of a third NFI member, NFIX, remains unknown. Here, we reveal that ventricular zone progenitor cells within the spinal cord express NFIX after the onset of NFIA and NFIB expression, and after the gliogenic switch has occurred. Mice lacking NFIX exhibit normal neurogenesis within the spinal cord, and, while early astrocytic differentiation proceeds normally, aspects of terminal astrocytic differentiation are impaired. Finally, we report that, in the absence of *Nfia* or *Nfib*, there is a marked reduction in the spinal cord expression of NFIX, and that NFIB can transcriptionally activate *Nfix* expression *in vitro*. These data demonstrate that NFIX is part of the downstream transcriptional program through which NFIA and NFIB coordinate gliogenesis within the spinal cord. This hierarchical organisation of NFI protein expression and function during spinal cord gliogenesis reveals a previously unrecognised auto-regulatory mechanism within this gene family.

1. Introduction

The generation of cellular identity and diversity within the developing central nervous system is dependent on networks of gene expression controlled by transcription factors (Stolt and Wegner, 2010). For instance, within the developing spinal cord the asymmetric division of neural progenitor cells within the ventricular zone (VZ) first generates neurons. This occurs from approximately embryonic day (E) 9 in mice (Butler and Bronner, 2015). Diverse neuronal populations are produced along the dorso-ventral axis of the spinal cord as a result of the spatially restricted expression of homeodomain-containing transcription factors including PAX6 and NKX2.2 (Briscoe et al., 2000, 1999; Ericson et al., 1997). This patterning arises as a result of the diffusion of morphogens such as sonic hedgehog, which is expressed in the notochord and floorplate (Ericson et al., 1997). At approximately E11.5 in mice, a process dubbed the 'gliogenic switch' occurs (Kang et al., 2012), such that the production of neurons following the division of neural progenitor cells declines, and instead glia (astrocytes and oligodendrocytes) begin to be produced. Again, this process is reliant on tightly regulated transcriptional networks coordinated by factors such as SOX8 and SOX9, as mice lacking these genes exhibit deficits in glial fate specification within the spinal cord (Stolt and Wegner, 2010).

Transcription factors from the nuclear factor I (NFI) family have also been implicated in coordinating gliogenesis within the spinal cord (Deneen et al., 2006; Kang et al., 2012). This family, comprising NFIA, NFIB, NFIC and NFIX, is broadly expressed within the developing nervous system and elsewhere within the embryo (Barry et al., 2008; Chaudhry et al., 1997; Mason et al., 2009). Within the spinal cord, expression of NFIA and NFIB is initiated between E11.5 and E12.5 within neural progenitor cells, coinciding with the gliogenic switch (Deneen et al., 2006). Moreover, both loss-of-function and gain-of-function studies have revealed that NFIA and NFIB play an instructive role in the gliogenic switch, by both inhibiting neurogenesis, and initiating a program of gliogenesis within spinal cord neural progenitor cells (Deneen et al., 2006). More recently, NFIA has been shown to act in concert with SOX9 to promote astrocyte development within the embryonic spinal cord, in part through the transcriptional regulation of

* Corresponding author at: School of Biomedical Sciences, The University of Queensland, Brisbane, Qld 4072, Australia.
E-mail address: m.piper@uq.edu.au (M. Piper).
[1] These authors contributed equally to this work.

http://dx.doi.org/10.1016/j.ydbio.2017.10.019
Received 4 May 2017; Received in revised form 23 October 2017; Accepted 23 October 2017
Available online 26 October 2017
0012-1606/

genes such as *Apcdd1* and *Mmd2* (Kang et al., 2012).

NFIX has also been shown to be vital for the differentiation of neural progenitor cells within the embryonic, postnatal and adult brain (Harris et al., 2013, 2015). For example, NFIX expression within radial glial progenitors in the dorsal telencephalon has been shown to play a role in repressing stem cell self-renewal genes such as *Sox9*, while activating inscuteable gene expression to promote the production of intermediate neuronal progenitors (Harris et al., 2016; Heng et al., 2014). *In vitro*, NFIX has been shown to activate the transcription of astrocytic genes (Singh et al., 2011b), work that is supported by the delay in gliogenesis exhibited by *Nfix*$^{-/-}$ mice within the forebrain (Heng et al., 2014) and cerebellum (Piper et al., 2011). However, whether or not NFIX plays a role in the gliogenic switch during spinal cord development has yet to be addressed. Moreover, the transcriptional regulation of the *Nfix* gene itself is poorly characterised. Here, we reveal that NFIX expression is initiated in neural progenitor cells within the developing mouse spinal cord at E13.5, subsequent to NFIA and NFIB and after the gliogenic switch. NFIX expression is downregulated in both *Nfia*$^{-/-}$ and *Nfib*$^{-/-}$ mice, but only NFIB can activate *Nfix*-promoter driven transcription *in vitro via* the promoter regions we analysed, suggesting that NFIX is a direct downstream target of NFIB during spinal cord development. In support of this, embryonic terminal glial differentiation is impaired in the absence of *Nfix*, while neuronal differentiation and aspects of early glial differentiation occur normally. Collectively, these data highlight the importance of the *Nfi* family in promoting timely gliogenesis within the spinal cord.

2. Methods

2.1. Animals and genotyping

Nfix$^{-/-}$ (Campbell et al., 2008), *Nfia*$^{-/-}$ (das Neves et al., 1999) and *Nfib*$^{-/-}$ mice (Steele-Perkins et al., 2005) were used in this study, along with wild-type littermates. All strains were maintained on a C57Bl/6J background. Timed-pregnant females were obtained by placing heterozygous male and female mice together overnight. The presence of a vaginal plug the following day was designated as embryonic day (E)0.5. The genotype of each mouse was confirmed by polymerase chain reaction (PCR). Primer sequences are available upon request. Wild-type C57Bl/6J animals were also used to perform chromatin immunoprecitipation. All animal procedures were performed with the approval of the University of Queensland animal ethics committee (QBI/353/13/NHMRC; QBI/383/16) and experiments were carried out in accordance with the Australian Code of Practice for the Care and Use of Animals for Scientific Purposes.

2.2. Tissue preparation, immunohistochemistry and immunofluorescence

Embryos were drop-fixed until E14.5 in 4% paraformaldehyde (PFA) or perfused transcardially at older ages with phosphate-buffered saline (PBS), followed by 4% PFA, then post-fixed for 48–72 h before long-term storage in PBS at 4 °C. Spinal cords were embedded in 3% noble agar and sectioned transversely using a vibratome at a thickness of 50 µm. Sections were mounted on Superfrost slides before immersion in 10 mM sodium-citrate solution and heat-mediated antigen retrieval at 95 °C for 15 min. Chromogenic immunohistochemistry (IHC) using 3,3′-diaminobenzidine (DAB), or fluorescence immunohistochemistry (IF) were then performed as previously described (Harris et al., 2013, 2017; Piper et al., 2009). The antibodies used and their details are listed in Table 1.

2.3. Image acquisition and analysis

Brightfield images of sections labelled with DAB were captured using an Axio Imager Z2 upright microscope (Zeiss) fitted with an Axio-Cam HRc camera. Image acquisition was performed using AxioVision software (Zeiss). Sections labelled with fluorescent antibodies were captured using a Diskovery inverted spinning-disk confocal system (Spectral Applied Research) consisting of a Ti-E microscope (Nikon) equipped with a Diskovery disk head (Spectral Applied Research), two Flash4.0 sCMOS cameras (Hamamatsu Photonics), and a 20× 0.75 NA CFI PlanApo objective. Five 2 µm thick optical sections were taken consecutively to generate 10 µm z-stacks. Fluorescence images of GFAP were captured using the Axio Imager Z2 upright microscope. Image acquisition was performed using NIS software (Nikon). All imaging work was performed in the Queensland Brain Institute's Advanced Microscopy Facility.

For GFAP IF analyses, 5 biological replicates were used with sections sampled from matching positions along the rostro-caudal axis and quantified blind to the genotype. Data was pooled from all locations along the rostro-caudal axis for statistical analysis. For NFIX IF analyses in *Nfia*$^{-/-}$ or *Nfib*$^{-/-}$ sections, and NFIB IF analyses in *Nfia*$^{-/-}$ sections, a minimum of 3 biological replicates were used, sampling from the spinal cord as above. Relative fluorescence intensities of protein stain were measured using integrated density; where integrated density = mean grey value of the area selected within the cell. To quantify NFIX or NFIB fluorescence intensity, the cells positive for these antibodies in each section and region of interest were outlined using the Otsu threshold method in Fiji Image J (open source) and the integrated density measurements were recorded. Areas of interest included the central canal and surrounding proximal region, as well as the migrating cell population observed towards the dorsal horn regions.

In order to limit variability, antibody staining performed for quantitative purposes were carried out on the same day, using the same antibody master mix. In addition, image acquisition for these samples was performed with identical settings on the same microscope, on the same day. Quantification, image analyses and processing were all performed using a combination of Adobe Photoshop CS5.1 (Adobe Systems Inc.) and Fiji Image J (open source) programs.

2.4. Quantitative PCR (qPCR) data and analysis

1 µg of total RNA was isolated from E14.5 spinal cords using an RNeasy micro isolation kit (QIAGEN) and reverse transcribed to cDNA. qPCR was performed with using SYBR Green Master Mix 2x (QIAGEN) and a LightCycler 480 machine (Roche). Primer sequences are listed in Table 2. To calculate the relative changes in gene expression the housekeeping gene *glyceraldehyde 3-phosphate dehydrogenase* (*Gapdh*) was used to normalize all samples using the $2^{-\Delta\Delta Ct}$ method (Yuan et al., 2006). All individual samples were run in triplicate during each experiment, in addition to a minimum of 4 biological replicates.

2.5. Luciferase reporter assay

Analysis of a published chromatin immunoprecipitation and sequencing (ChIP-seq) dataset in which a pan-NFI antibody was used on embryonic stem cell-derived neural stem cell cultures (Mateo et al., 2015), revealed two putative ChIP peaks within the *Nfix* promoter region, one at the transcriptional start site (TSS; Chromosome 8: 87297728–87298821, mm9) and another 4637 base pairs upstream of the TSS (Chromosome 8: 87302652–87302905, mm9). As such, two different luciferase reporter constructs containing these sites were generated.

The first of these luciferase constructs contained a 1234 base pair fragment of the mouse *Nfix* promoter region encompassing the location of the ChIP peak closest to the TSS (Mateo et al., 2015) and the basal promoter of the *Nfix* gene (Chromosome 8: 87297440–87298673, mm9), which was cloned upstream of the Renilla luciferase gene in a pLightSwitch_Prom reporter vector (Switchgear Genomics; *Nfix* pLUC). The second of these luciferase constructs contained a 1078

Table 1
Primary and secondary antibodies used for immunohistochemistry (IHC) and immunofluorescence (IF).

Antibody	Host	Use	Dilution	Source
Primary Antibodies				
GFAP	Rabbit polyclonal	IF	1:500	Dako, Z0334
GLAST	Rabbit polyclonal	IHC	1:10,000	Gift from Dr Neils Danbolt, University of Oslo
IBA1	Goat polyclonal	IF	1:250	Abcam, ab5076
Ki67 (FITC clone SolA15)	Mouse monoclonal	IF	1:400	Ebioscience,11–5698-80
NeuN	Mouse monoclonal	IHC	1:150	Millipore, MAB377
NeuN	Rabbit monoclonal	IF	1:400	Abcam, ab177487
NFIA	Rabbit polyclonal	IHC	1:500	Millipore, HPA008884
NFIB	Rabbit polyclonal	IHC	1:500	Sigma-Aldrich, HPA003956
NFIX	Rabbit polyclonal	IHC	1:500	Abcam, AB101341
NFIX (clone 3D2)	Mouse monoclonal	IF	1:100	Sigma-Aldrich, SAB1401263
OLIG2	Rabbit polyclonal	IF	1:300	Millipore, AB9610
SOX2	Rabbit polyclonal	IHC	1:250	Cell Signalling Technology, AB2758
SOX2 (Alexa Fluor 488)	Mouse monoclonal	IF	1:250	eBioscience, 53–9811,
SOX9	Rabbit polyclonal	IF	1:200	Merck, AB5535
Secondary antibodies				
Alexa Fluor 488	Goat anti-rabbit	IF	1:250	Abcam, ab150113
Alexa Fluor 647	Donkey anti-mouse	IF	1:250	Abcam, ab150107
488	Donkey anti-goat	IF	1:250	Thermo Fisher, A–11055
488	Goat anti-mouse	IF	1:250	Thermo Fisher, A–11001
Alexa Fluor 647	Goat anti-rabbit	IF	1:250	Thermo Fisher, A–21240
Cy3 FAB	Mouse	IF	1:250	Jackson Immunoresearch, 015–160-007
IgG	Biotinylated donkey anti-mouse	IHC	1:1000	Jackson Immunoresearch, 715–065-150
IgG	Biotinylated goat anti-rabbit	IHC	1:1000	Vector Laboratories, BA-1000

Table 2
The qPCR primers used for the quantification of transcriptional levels in *Nfix*$^{-/-}$ and wild-type mice.

Primer name	Sequence 5′ - 3′
Aldh1l1 For	TCACAGAAGTCTAACCTGCC
Aldh1l1 Rev	AGTGACGGGTGATAGATGAT
Aqp4 For	TATCCAGTGGTTTGCCCAGT
Aqp4 Rev	GCAATTGGACATTTGTTTGC
Blbp (Fabp7) For	TGGGAAACGTGACCAAACCA
Blbp (Fabp7) Rev	AGCTTGTCTCCATCCAACCG
CD44 For	AGCGGCAGGTTACATTCAAA
CD44 Rev	CAAGTTTTGGTGGCACACAG
Fgfr3 For	CTCCTGCTGGCTAGGTTCAG
Fgfr3 Rev	TCGTGGCTGGAGCTACTTC
Gapdh For	GCACAGTCAAGGCCGAGAAT
Gapdh Rev	GCCTTCTCCATGGTGGTGAA
GlnS (Glul) For	TTATGGGAACAGACGGCCAC
GlnS (Glul) Rev	AAAGTCTTCGCACACCCGAT
Mki67 (Ki67) For	TGCAAAGGTAGAGGCTCCAT
Mki67 (Ki67) Rev	CAGGTAGGCCAGAGCAAGT
Olig2 For	CAGAGCCAGGTTCTCCTCC
Olig2 Rev	CCCCAGGGATGATCTAAGC
Rbfox3 (NeuN) For	ATGGTGCTGAGATTTATGGAGG
Rbfox3 (NeuN) Rev	CCGATGGTGTGATGGTAAGG
S100b For	ACATCAATGAGGGCAACCAT
S100b Rev	GGACACTGAAGCCAGAGAGG
Slc1a2 (Glt-1) For	GGAGCTGAGGTGGCTGTC
Slc1a2 (Glt-1) Rev	CAGAAGTTGGAAGCCAGTGC
Slc1a3 (Glast) For	CACTGCTGTCATTGTGGGTA
Slc1a3 (Glast) Rev	AGCATCCTCATGAGAAGCTC
Sox2 For	CCAATCCCATCCAAATTAACGC
Sox2 Rev	CTATACATGGTCCGATTCCCC
Sox9 For	TCCACGAAGGGTCTCTTCTC
Sox9 Rev	AGGAAGCTGGCAGACCAGTA

base pair fragment encompassing the region of the more distal peak (Chromosome 8: 87323676–87324754, mm9) and cloned upstream of the Renilla luciferase gene in the long-range enhancer reporter vector containing a basal promoter, pLightSwitch_LR (Switchgear Genomics).

Overexpression vectors used in the luciferase assays were *Nfia* or *Nfib* full-length cDNA driven by a CMV early enhancer/chicken β-actin promoter and splice acceptor rabbit β-globin (*Nfia* pCAGIG, *Nfib* pCAGIG and an empty vector control pCAGIG) (Matsuda and Cepko, 2004). Cells from the neuroblastoma cell line, Neuro2A, or the astrocytoma cell line, U251, were seeded at 1×10^4 cells per well in a 96-well plate 24 h prior to transfection. DNA was transfected with one of the above luciferase reporter and overexpression constructs using Lipofectamine 2000 (Thermo Fisher). Each transfection had Cypridina (Switchgear Genomics) added as an internal control for normalization. Luciferase activity was measured at 24 h post-transfection using a dual-luciferase system (Switchgear Genomics). Each condition was performed in triplicate, and the experiment was repeated five times.

2.6. Chromatin immunoprecipitation (ChIP) and qPCR assay

E14.5 C57Bl/6J wild-type mouse spinal cords were dissected and homogenized, and cross-linked chromatin was sheared *via* sonication for use in the ChIP-qPCR assays. ChIP was performed on the sheared chromatin with anti-NFIA (HPA008884, Sigma-Aldrich) and anti-NFIB (HPA003956, Sigma-Aldrich) antibodies, as well as the control antibodies H3K27ac (AB4729, Abcam; positive control) and Rb IgG (AB171870, Abcam; negative control) coupled to 30 µl of magnetic Protein G Dynabeads (Thermo Fisher). The qPCR of the samples was performed with the primer sets listed in Table 3, SYBR Green Master Mix 2x (QIAGEN) and a LightCycler 480 machine (Roche). All

Table 3
ChIP-qPCR primers used to analyse the binding of NFIA and NFIB to the *Nfix* promoter and control regions.

Primer name	Sequence 5′ - 3′
Positive control For	CTGTCACCAACCTGACGGT
Positive control Rev	CAGAACCAAGTGGACAG
Negative control For	GATTGCAGAGTAAGATCCCTT
Negative control Rev	GCGTAAGTTCTACATGCTGCT
Proximal Set #1 For	ACTTGTCGATTGGGCAAATTGT
Proximal Set #1 Rev	AAAGAGGCATCCACTTGCAGC
Proximal Set #2 For	CAATCCTAGTGTTCCCACCCC
Proximal Set #2 Rev	AACAAGCGAAGTCCAGCAGT
Distal Set #1 For	GGAATGTGGGGGATTCCAGC
Distal Set #1 Rev	GTACCCCATTTTCCTGTCTCCC
Distal Set #2 For	TGCTGGATGTATGCCCACTT
Distal Set #2 Rev	GGGAGGGAGGGCCTAAACAT
mId4 For Primer	CTAGGCTGTGTCTGAAGCAC
mId4 Rev Primer	ACTCTCCTACAAGCTGGCAC

individual samples were run in triplicate during each experiment, in addition to a minimum of 4 biological replicates.

2.7. Statistical analyses

One-sided unpaired non-parametric Mann-Whitney tests were performed for statistical analysis when comparing two groups with n = 3. Two-tailed unpaired *t*-tests were used for statistical analyses in groups with n > 3. For experiments in which there were more than two independent variables, a two-way ANOVA was performed followed by a Tukey's multiple comparisons test. Significance was determined at a p value ≤ 0.05 and error bars in figures represent the standard error of the mean (SEM).

3. Results

3.1. Expression pattern of NFIX during spinal cord development

While it has been established that both NFIA and NFIB are key factors in driving the gliogenic switch within the developing spinal cord (Deneen et al., 2006), the spatial and temporal dynamics of NFIX expression and its functional significance within the same context has yet to be examined. Consistent with previous reports, we found that NFIA and NFIB were expressed within neural progenitor cells located in the spinal cord VZ from approximately E11.5 to E12.5 (Deneen et al., 2006) (Fig. 1B, B′, C and C′). The timing of the expression of these transcription factors coincided with that of GLAST, a marker for astrocyte precursors and the onset of gliogenesis (Shibata et al., 1997) (Fig. 1D and D′). NFIX expression however, was not observed within the neural progenitor cell population of the spinal cord until after the gliogenic switch had occurred, after E12.5 (Fig. 1A, A′, E and E′). To map the dynamics of NFIX expression more closely, immunohistochemistry was performed on spinal cord sections from mice of different embryonic ages, ranging from E13.5 to E18.5. NFIX expression was first observed at E13.5 within the cell population lining the central canal (Fig. 2A, A′). Expression of NFIX within these cells became the most apparent between E14.5 and E15.5, but was also observed in cells both adjacent to and migrating away from the central canal towards the dorsal horn regions (Fig. 2B, B′, C and C′). At later embryonic ages the expression of NFIX became less pronounced but was still evident in the VZ and by cells scattered throughout the spinal cord (Fig. 2D, D′, E and E′).

To verify the expression of NFIX by neural progenitor cells surrounding the central canal, co-immunofluorescence (co-IF) was performed through the labelling of E14.5 spinal cord sections with the progenitor marker SOX2 (Ellis et al., 2004). Analysis of sections *via* confocal microscopy revealed that SOX2-expressing neural progenitor cells were immunopositive for NFIX within the VZ (Fig. 3A-D). Interestingly, NFIX expression was higher in the neural progenitor

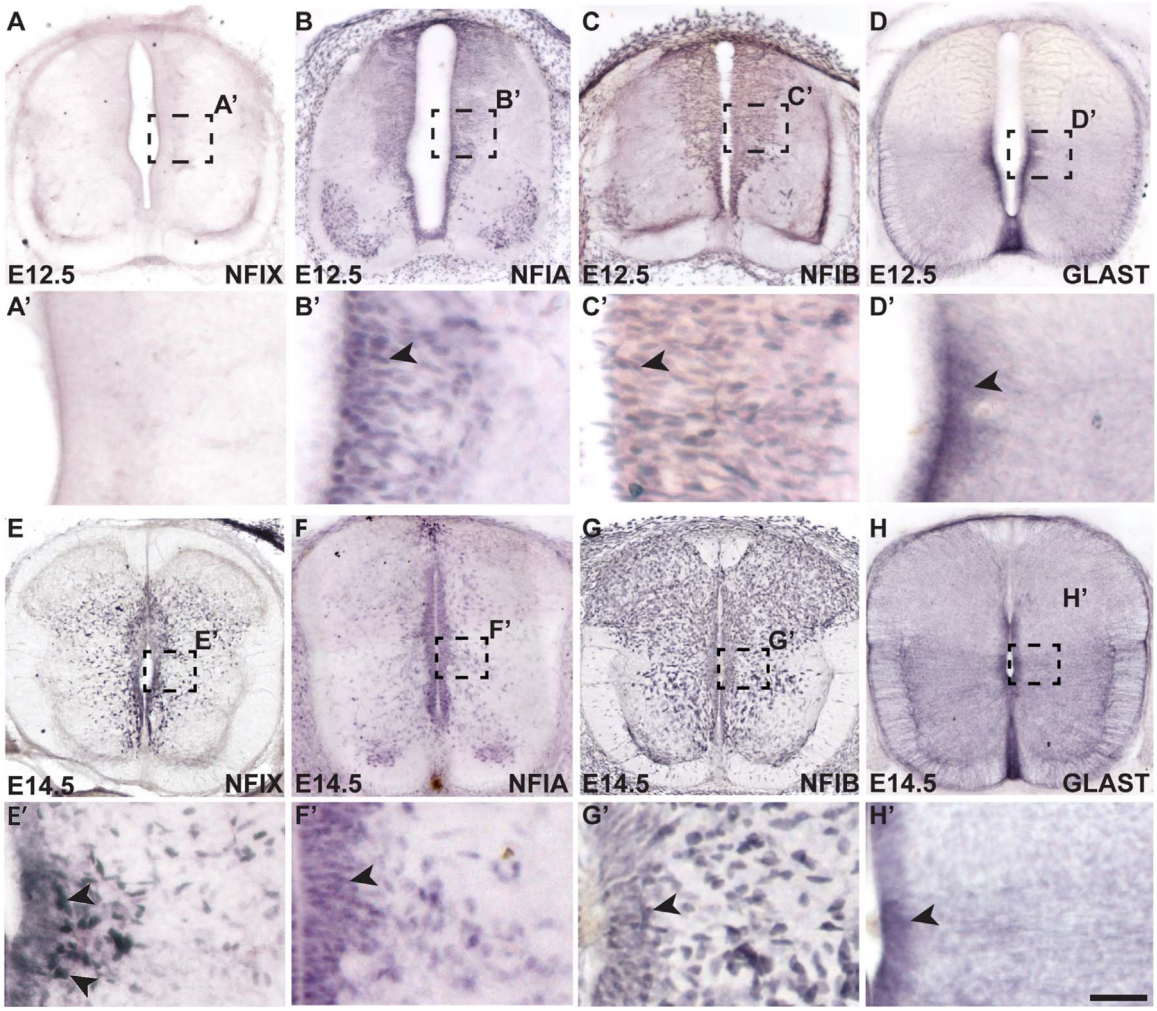

Fig. 1. NFIX is expressed after the gliogenic switch in the embryonic spinal cord. Transverse sections of wild-type spinal cords at ages E12.5 (A-D′) and E14.5 (E-H′) were stained for NFIA, NFIB NFIX, and a marker of early gliogenesis, GLAST. Boxed regions in A-D and E-H are shown in A′-D′ and E′-H′ respectively. (A, A′) At E12.5, NFIX expression was not observed. (E, E′) However, at E14.5 NFIX expression was observed in and around the ventricular zone of the spinal cord (arrowheads in E′). This expression pattern occurs after NFIA (arrowheads in B′, F′), NFIB (arrowheads in C′, G′) and GLAST expression (arrowheads in D′, H′). Scale bar (in H′): A-H = 200 μm; A′-H′ = 50 μm.

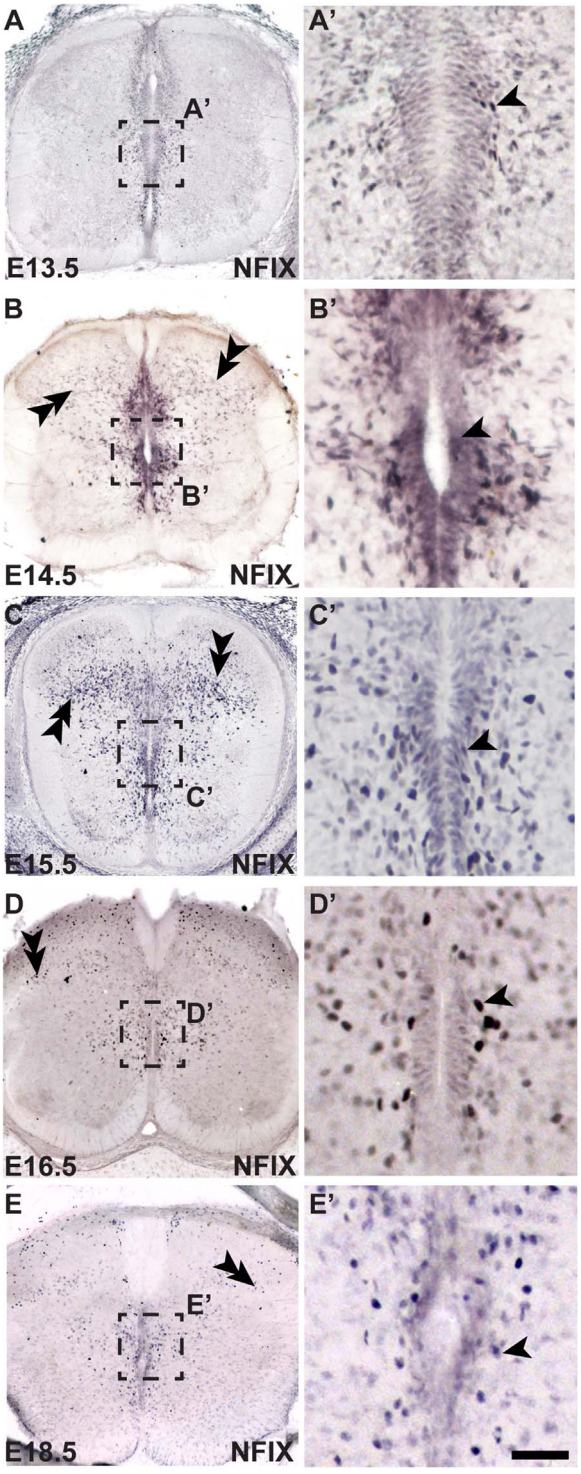

Fig. 2. NFIX is expressed within the ventricular zone, and later, the dorsal horn region of the developing spinal cord. NFIX expression in transverse sections of E13.5 to E18.5 wild-type spinal cords. (A) NFIX was first detected at E13.5 in the cells surrounding the central canal of the spinal cord (arrowhead in A′). At E14.5 (B, B′) and E15.5 (C, C′), NFIX expression was evident within the ventricular zone (arrowheads in B′, C′) as well as by cells within the dorsal horn (double arrowheads in B, C). NFIX expression decreased by E16.5 (D, D′) and E18.5 (E, E′), but was still present at low levels around the ventricular zone (arrowheads in D′, E′) and sparsely scattered cells throughout the rest of the spinal cord (double arrowheads in D, E). Scale bar (in E′): A-E = 200 μm; A′-E′ = 70 μm.

cells located on the ventral side of the VZ, perhaps reflecting the early patterning of glial precursors in the ventral neural tube coordinated by gradients of a variety of morphogens and transcription factors

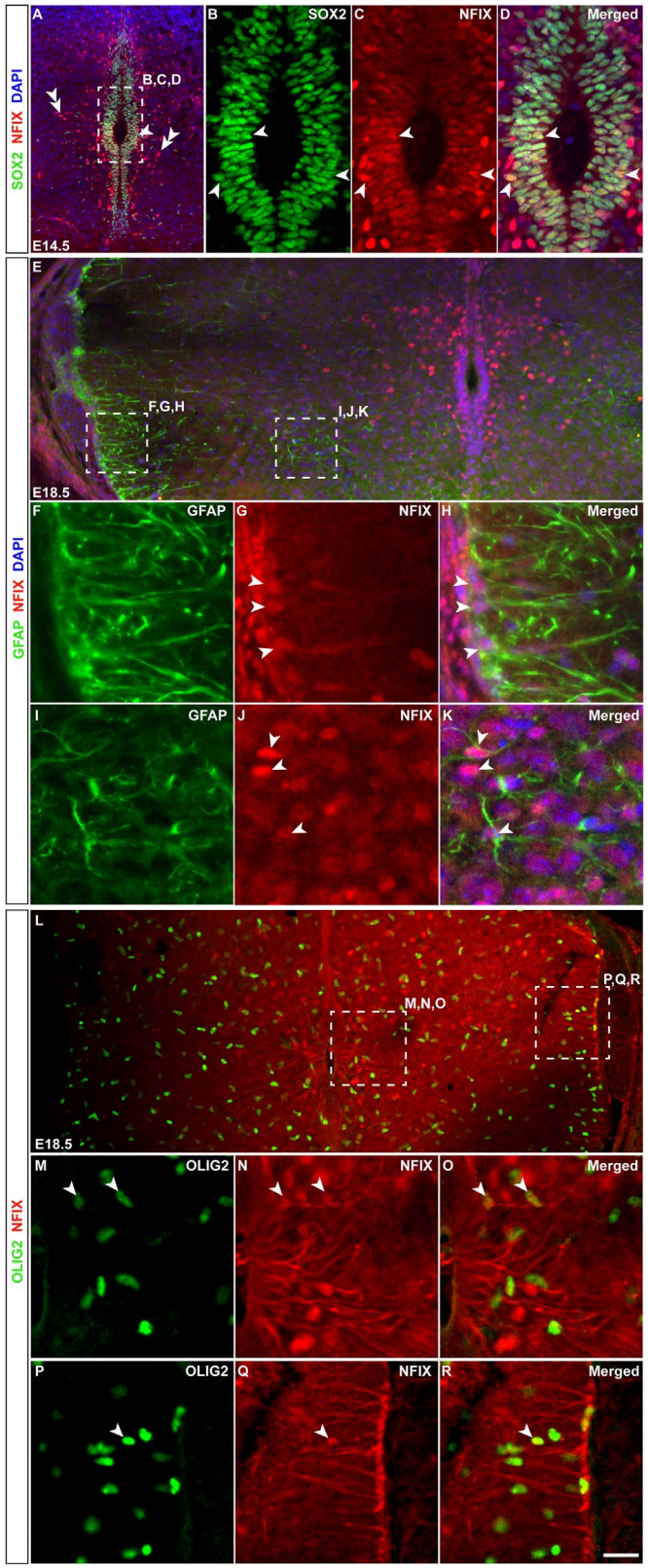

Fig. 3. Neural progenitor cells and astrocytes express NFIX within the developing spinal cord. (A-D) A transverse section of an embryonic spinal cord from an E14.5 wild-type mouse at both a low (A) and high (B-D) magnification, labelled with the nuclear marker DAPI (blue), the neural progenitor cell marker SOX2 (green), and NFIX (red). The boxed region in A indicates the location of the higher power images of the ventricular zone in B-D. The majority of SOX2-positive cells lining the central canal expressed NFIX (arrowheads), with cells lining the ventral side of the ventricular zone exhibiting the highest expression. NFIX-expressing cells were also observed within the mantle zone of the spinal cord (double arrowheads in A). (E-K) Transverse section of a spinal cord from an

E18.5 wild-type mouse at both a low (E) and high (F-K) magnification, labelled with the nuclear marker DAPI (blue), the mature astrocyte marker GFAP (green), and NFIX (red). The boxed regions in E indicate the locations of the higher power images in F-H and I-K. Mature astrocytes lining the periphery of the spinal cord express NFIX (F-H; arrowheads), as do astrocytes within the mantle zone (I-K; arrowheads). (L-R) Transverse section of a spinal cord from an E18.5 wild-type mouse at both a low (L) and high (M-R) magnification, labelled with DAPI (blue), OLIG2 (green), and NFIX (red). The boxed regions in L indicate the locations of the higher power images in M-O and P-R. A subset of OLIG2-expressing cells expressed NFIX near the central canal (arrowheads in M-O) and at the periphery of the spinal cord (arrowheads in P-R). Scale bar (in R): A = 200 μm; B-D = 50 μm; E, L = 250 μm; F-K, M-R = 25 μm.

(Hochstim et al., 2008; Rowitch, 2004). Expression of NFIX by progenitor cells within the embryonic spinal cord was further supported by the co-expression of NFIX and SOX9 within ventricular zone progenitor cells (Supp. Fig. 1A-D). NFIX-expressing cells positioned outside of the VZ were negative for SOX2 (Fig. 3A), suggesting these were more differentiated cell types. Indeed, we detected co-expression of NFIX and SOX9 by cells within the mantle zone and spinal cord periphery at E18.5 (Supp. Fig. 1E-K), suggesting that NFIX could be expressed by cells of the astrocytic lineage. Consistent with this, NFIX expression was detected in glial fibrillary acidic protein (GFAP)-expressing astrocytes in the late gestation spinal cord (Fig. 3E). These cells were located at the periphery of the spinal cord (Fig. 3F-H), as well as in the mantle layer (Fig. 3I-K). Consistent with expression of NFIX within the adult forebrain (Chen et al., 2017), NFIX expression was also detected within a small subset of neurons (Supp. Fig. 2), and by a subpopulation of OLIG2-expressing cells of the oligodendrocyte lineage (Fig. 3L-R). We did not observe co-expression of NFIX with the microglial marker IBA1 (data not shown).

3.1.1. *Nfix*$^{-/-}$ mice display no changes in neurogenesis

Given the expression of NFIX by spinal cord neural progenitor cells, we examined whether the absence of *Nfix* has a similar effect on this population of progenitors as seen in other regions of the developing CNS, such as the hippocampus, in which there is prolonged proliferation of the progenitor pool (Harris et al., 2016; Heng et al., 2014). We performed IHC on the spinal cords of *Nfix*$^{-/-}$ mice and their wild-type littermate controls, between E14.5 and E16.5 using antibodies for SOX2 and Ki67. There was no significant difference in the number of cells expressing the proliferative marker Ki67 in the VZ of *Nfix*$^{-/-}$ mice compared to controls, nor the neural progenitor marker, SOX2 (Supp. Fig. 3). In support of these observations, qPCR performed on cDNA derived from the spinal cord of E14.5 *Nfix*$^{-/-}$ mice revealed no changes in expression for either of these genes at a transcriptional level (Supp. Fig. 3C, F). Together, these data indicate that NFIX does not play a major role in the maintenance of spinal cord progenitor cell population, or its continued proliferation.

In light of these findings, and the fact that NFIX is expressed after the majority of spinal cord neurons are generated (Caspary and Anderson, 2003), we hypothesised that the deletion of *Nfix* would also have no effect on neuronal production. Neurogenesis was assessed *via* immunohistochemistry for the expression of a neuronal marker, NeuN (RBFOX3), in *Nfix*$^{-/-}$ and wild-type mice. Neurogenesis was normal in the spinal cord of embryonic *Nfix*$^{-/-}$ mice with regards to cell numbers, cellular appearance and distribution of NeuN-positive cells in the spinal cord grey matter (Supp. Fig. 4A-F, H). In addition, there was no difference in the mRNA levels of *Rbfox3* when assessed at E14.5 in *Nfix*$^{-/-}$ spinal cord tissue compared to wild-type mice (Supp. Fig. 4G). This is in contrast to the role of NFIX within the developing hippocampus, where the production of intermediate neuronal progenitors, and subsequent neurogenesis, is delayed in *Nfix*$^{-/-}$ mice (Harris et al., 2016; Heng et al., 2014). Similarly, in the cerebellum, granule neuron progenitors exhibit impaired migration and axon outgrowth in the absence of *Nfi* genes, including *Nfix* (Piper et al., 2011; Wang et al., 2007). These data highlight the context-specific roles of NFIX during nervous system development.

3.1.2. *Nfix*$^{-/-}$ mice display a transient delay in oligodendrocyte production

NFI family members have previously been implicated in different aspects of oligodendrogenesis. NFIB, for instance, has been implicated in promoting oligodendrocyte production in the adult hippocampus (Rolando et al., 2016) and NFIA has been implicated in specifying the oligodendrocytic lineage during early phases of gliogenesis within both the nascent mouse spinal cord (Deneen, 2006), and the postnatal forebrain (Wong et al., 2007). In contrast, NFIX has been reported to suppress oligodendrogenesis both *in vitro*, and within postnatal subventricular zone stem cells from the mouse forebrain (Zhou et al., 2015). Given the strong expression of NFIX by neural progenitor cells within the spinal cord central canal at E14.5 (Fig. 3A-D), we investigated whether the loss of NFIX could enhance the production of oligodendrocytes. To address this question, we analysed the expression of the oligodendrocyte-lineage marker, OLIG2 (Yokoo et al., 2004) in wild-type and *Nfix*$^{-/-}$ tissue at ages between E14.5 and E16.5. In contrast to the forebrain, we saw a delay in oligodendrocyte production at E14.5, but saw no significant difference in spinal cord oligodendrocyte formation in the *Nfix*$^{-/-}$ mice, both in regards to the number of OLIG2-immunopositive cells and their distribution at E15.5 and E16.5 (Supp. Fig. 5A-F, H). Moreover, no difference in *Olig2* expression was found at the transcriptional level (Supp. Fig. 5G). These data suggest that, despite being expressed by a sub-population of OLIG2-positive cells, the loss of *Nfix* does not bias neural progenitor cells to generate oligodendrocytes, further highlighting the fact that the role of NFIX in forebrain development is not fully recapitulated within the developing spinal cord.

3.1.3. *Nfix*$^{-/-}$ mice display delayed terminal astrocytic differentiation

One role of NFIs that has been consistently observed, both *in vitro*, and *in vivo* in various regions of the brain, including the cerebellum, neocortex and hippocampus, is the capacity to promote astrocytic differentiation (Harris et al., 2016; Heng et al., 2014; Piper et al., 2011; Singh et al., 2011b; Wilczynska et al., 2009). As such, we analysed astrocytic development in *Nfix*$^{-/-}$ mice. Unlike mice lacking *Nfia* or *Nfib* (Deneen et al., 2006), we found that the expression of GLAST was not diminished in the absence of *Nfix* in the spinal cord, as the expression and distribution of this marker in the mutant was comparable to the control between E14.5 to E16.5 at both protein (Fig. 4A-F) and mRNA levels (Fig. 4G). Again, these findings highlight fundamental differences in the role of NFIX in the dorsal forebrain (Heng et al., 2014) and spinal cord during development. These findings do not, however, preclude a role for NFIX in promoting astrocytic development. Indeed, previous work performed *in vitro* has suggested that NFIX may function later than NFIA and NFIB in promoting glial differentiation (Wilczynska et al., 2009). To determine if NFIX coordinates terminal glial differentiation, we analysed the expression of the mature astrocyte marker GFAP. Consistent with the finding that NFIX acts to drive later stages of glial differentiation *in vitro* (Wilczynska et al., 2009), the expression of GFAP was significantly diminished throughout the spinal cord of E18.5 mutant mice in comparison to wild-type controls (Fig. 4H-I and J). The expression of GFAP in the spinal cord of *Nfix*-deficient mice resembled that observed in mice lacking either *Nfia* or *Nfib* (Supp. Fig. 6A-D). Furthermore, the expression of *Gfap* mRNA was significantly reduced in *Nfix*$^{-/-}$ mice compared to controls (Fig. 4K). Additionally, we compared the expression of other astrocyte-specific markers in E18.5 *Nfix*$^{-/-}$ mice to wild-type controls using qPCR (Fig. 4L-N). Decreased mRNA expression was observed for *Aldh1l1* (Cahoy et al., 2008), *Glu1*, and *Aqp4* ($p = 0.058$) (Cahoy et al., 2008; Fallier-Becker et al., 2014). We saw no significant difference in the mRNA expression of other markers, including *Cd44, Fabp7, Fgf3* and *s100β*. In line with a role in promoting later stages of astrocytic maturation, the expression of *Sox9* mRNA was not significantly different in mice lacking *Nfix*. Interestingly, by postnatal day 10, the expression of GFAP within the spinal cord of *Nfix*$^{-/-}$ mice was

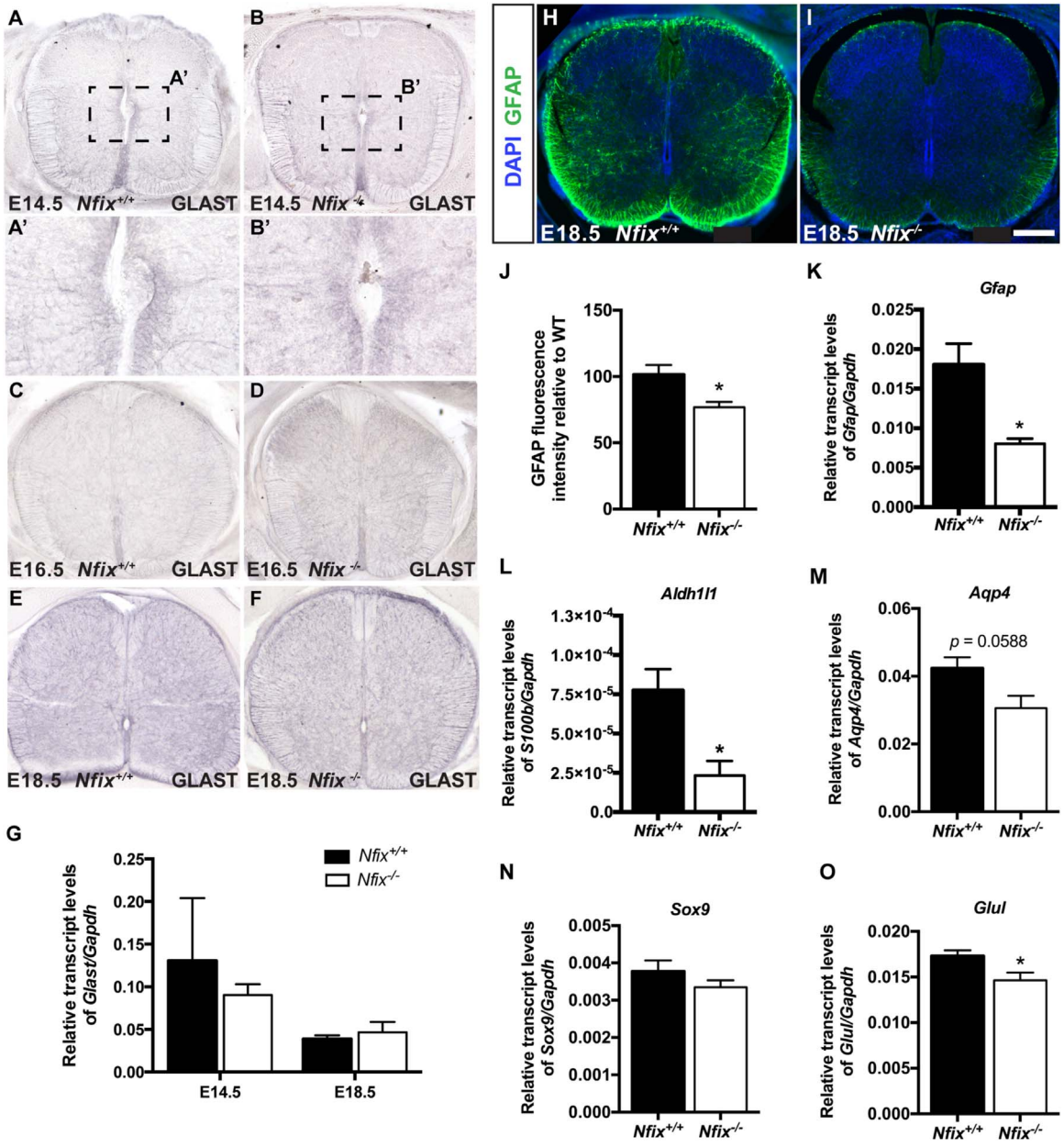

Fig. 4. *Nfix*$^{-/-}$ mice display a decrease in the expression of the mature astrocyte marker, GFAP, but not the early astrocyte marker GLAST. Transverse sections of spinal cords from E14.5 to E18.5 were taken from *Nfix*$^{-/-}$ and wild-type mice and stained for the early glial marker, GLAST. *Nfix*$^{-/-}$ mice (B, D and F) displayed no changes in the expression of early glial cell marker GLAST in comparison to control mice (A, C and E). Boxed regions in A and B are shown in A′ and B′ respectively. (G) No change in mRNA levels for *Glast* was detected at E14.5 or E18.5 in *Nfix*$^{-/-}$ mice compared to controls. (H-I, J) GFAP fluorescence intensity was reduced in the spinal cords of *Nfix*$^{-/-}$ mice at E18.5. (K) *Gfap* mRNA levels were also significantly reduced in the mutant at this age. (L-O) mRNA levels of additional markers of mature astrocytes such as *Aldh1l1, Glu1* and *Aqp4* were also reduced in *Nfix*$^{-/-}$ mice. No significant difference in the expression of *Sox9* was observed between wild-type and mutant mice at E18.5. Statistical analyses were performed with two-tailed unpaired *t*-tests (n = 4 for mRNA analyses, n = 5 for IFs). *$p \leq 0.05$. Scale bar in (I): A-F, H-I = 200 μm; A′-B′ = 80 μm.

comparable to that of the control when analysed *via* fluorescence intensity staining (Supp. Fig. 7A-C), indicative of the embryonic phenotype representing a delay in astrocyte differentiation, rather than an inability of these cells to mature. Furthermore, we saw no evidence for increased caspase-mediated cell death in the spinal cords of *Nfix* mutant mice at ages between E14.5 and E18.5 (data not shown). Collectively, the expression of NFIX by neural progenitor cells within the spinal cord at E13.5–15.5, coupled with the decrease in the expression of mature astrocyte markers within the late gestation spinal cord in the absence of *Nfix*, indicate that this transcription factor regulates terminal astrocytic differentiation. This finding is in stark contrast to other NFI family members, which act earlier to initiate the gliogenic switch, and to promote glial-lineage specification (Deneen et al., 2006). Critically, however, these findings corroborate a previous *in vitro* study of astrocyte differentiation in human neural progenitors that suggested individual NFIs may function in a temporally restricted manner such that NFIA and B act early in gliogenesis, whilst NFIX acts at a later phase of gliogenesis (Wilczynska et al., 2009).

3.1.4. NFIB binds to the Nfix promoter to drive its transcription

To this point, our findings have revealed that NFIX is expressed after NFIA and NFIB, and that aspects of terminal astrocytic differentiation are impaired in the absence of this transcription factor. One possibility arising from these findings is that *Nfix* is a downstream target of NFIA and/or NFIB during development of the spinal cord. However, very little is known regarding the control of the *Nfi* genes themselves within the developing central nervous system, with the

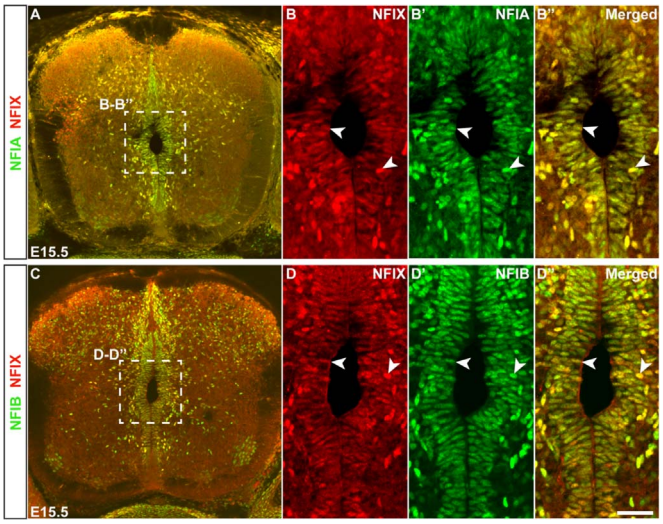

Fig. 5. NFIX co-localises with NFIA and NFIB within the developing spinal cord. Transverse sections of E15.5 wild-type spinal cords revealing to co-expression of NFIX (red) with NFIA (green; A, B-B") and NFIB (green; C, D-D") by ventricular zone progenitor cells (arrowheads in B-B" and D-D"). Scale bar in (D"): A, C 200 μm; B-B" and D-D" 50 μm.

exception of various microRNAs that have been implicated in the post-transcriptional regulation of *Nfi* gene expression *in vitro* (Fazi et al., 2005; Glasgow et al., 2013; Tsuyama et al., 2015). To investigate whether *Nfix* is a target for NFIA- and/or NFIB-mediated transcriptional activation, we first determined whether these factors are co-expressed by progenitor cells within the nascent spinal cord. To do this, we used anti-NFI antibodies whose specificity has previously been demonstrated in *Nfi* knockout tissue (Chen et al., 2017). Expression analysis at E15.5 revealed that progenitor cells within the spinal cord co-express NFIA and NFIX, as well as NFIB and NFIX, at this age (Fig. 5A-D). If NFIA or NFIB directly regulates *Nfix* expression, then these proteins will likely bind the promoter region of the *Nfix* gene. To identify potential NFI binding sites within the *Nfix* promoter, we analysed a recent ChIP-seq dataset that used a pan-NFI antibody to investigate genome-wide NFI occupancy within cultured neural stem cells derived from a mouse embryonic stem cell line (Mateo et al., 2015). This analysis identified two binding peaks within chromatin proximal to the *Nfix* transcriptional start site (TSS), indicating that NFIs may directly bind the *Nfix* promoter (Fig. 6A). One binding peak was detected at the TSS (−0TSS) within the promoter region, while the other peak was detected 4637 base pairs upstream (−4637 TSS), suggesting that *Nfix* may be transcriptionally regulated by NFI family members.

We next sought to determine if NFIA and/or NFIB occupy these sites within chromatin isolated from E14.5 spinal cord tissue. We used ChIP-qPCR to determine enrichment for NFIA or NFIB using primer sets spanning either the ChIP-peak region proximal to the *Nfix* TSS (proximal primer sets 1 and 2) or the upstream peak (distal primer sets 1 and 2; Fig. 6A). This approach revealed enrichment for NFIB occupancy at the ChIP-peak region within the *Nfix* proximal site (Fig. 6B). We did not observe any enrichment for NFIA binding at the proximal site, nor did we detect any significant enrichment for either NFIA or NFIB at the distal NFI ChIP-peak region (data not shown). Analysis of NFI occupancy at a different locus, MER130.31 corresponding to an *Id4* enhancer, demonstrated the capacity of this NFIA antibody to reveal enrichment of NFIA localisation within the genome (Supp. Fig. 8A), suggesting that the absence of NFIA enrichment at the *Nfix* promoter was not due to the inability of this antibody to recognise endogenous NFIA protein within this paradigm. Luciferase

A

NFI motif	Genomic co-ordinates of ChIP peaks	Genomic co-ordinates of primer sets	Length of sonicated chromatin
Distal to TSS			
5′- CTGGAAGAGCGCCTG -3′	Chromosome 8: 87302652-87302905, mm9	Distal set 1: 87302704-87302838	100-500bp
		Distal set 2: 87302458-87302588	100-500bp
Proximal to TSS			
5′- GAGGGAGACAGCCAG -3′	Chromosome 8: 87297728-87298821, mm9	Proximal set 1: 87298442-87298547	100-500bp
		Proximal set 2: 87298307-87298430	100-500bp

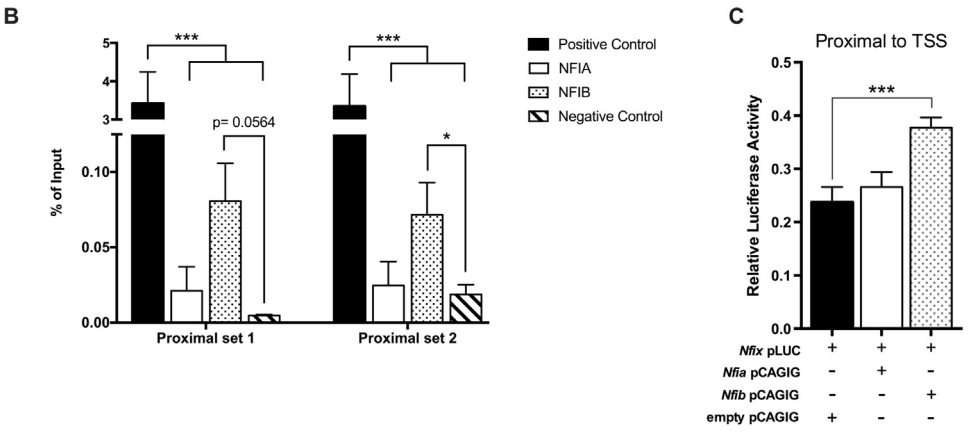

Fig. 6. NFIB directly regulates the transcription of *Nfix*. (A) ChIP qPCR primers were designed to overlap the binding-peak regions identified in a recent ChIP-seq dataset (Mateo et al., 2015). Distal primer sets 1 and 2 were designed to overlap with the distal binding motif, whereas proximal primer sets 1 and 2 were designed to overlap with the binding motif at the transcriptional start site (TSS). (B) ChIP qPCR of E14.5 mouse spinal cord tissue revealed enrichment of NFIB binding to the *Nfix* promoter using the primers proximal to the TSS, but not for NFIA binding. Neither NFIB nor NFIA were enriched in the chromatin region distal to the *Nfix* TSS (distal primer set 1 and 2, respectively; not shown). (C) A luciferase construct with an insert containing the ChIP peak region on the *Nfix* promoter proximal to the TSS (*Nfix* pLUC) was transfected into Neuro2A cells with either an NFIA (*Nfia* pCAGIG) or NFIB (*Nfib* pCAGIG) overexpression construct. The assay revealed an increase in *Nfix*-promoter driven *luciferase* transcription in cells that overexpressed NFIB but not NFIA. Statistical analyses were performed using two-way ANOVAs followed by a Tukey's multiple comparisons test (n = 4 for luciferase assays, and n = 4 for ChIP-qPCR). * $p \leq 0.05$; *** $p \leq 0.001$.

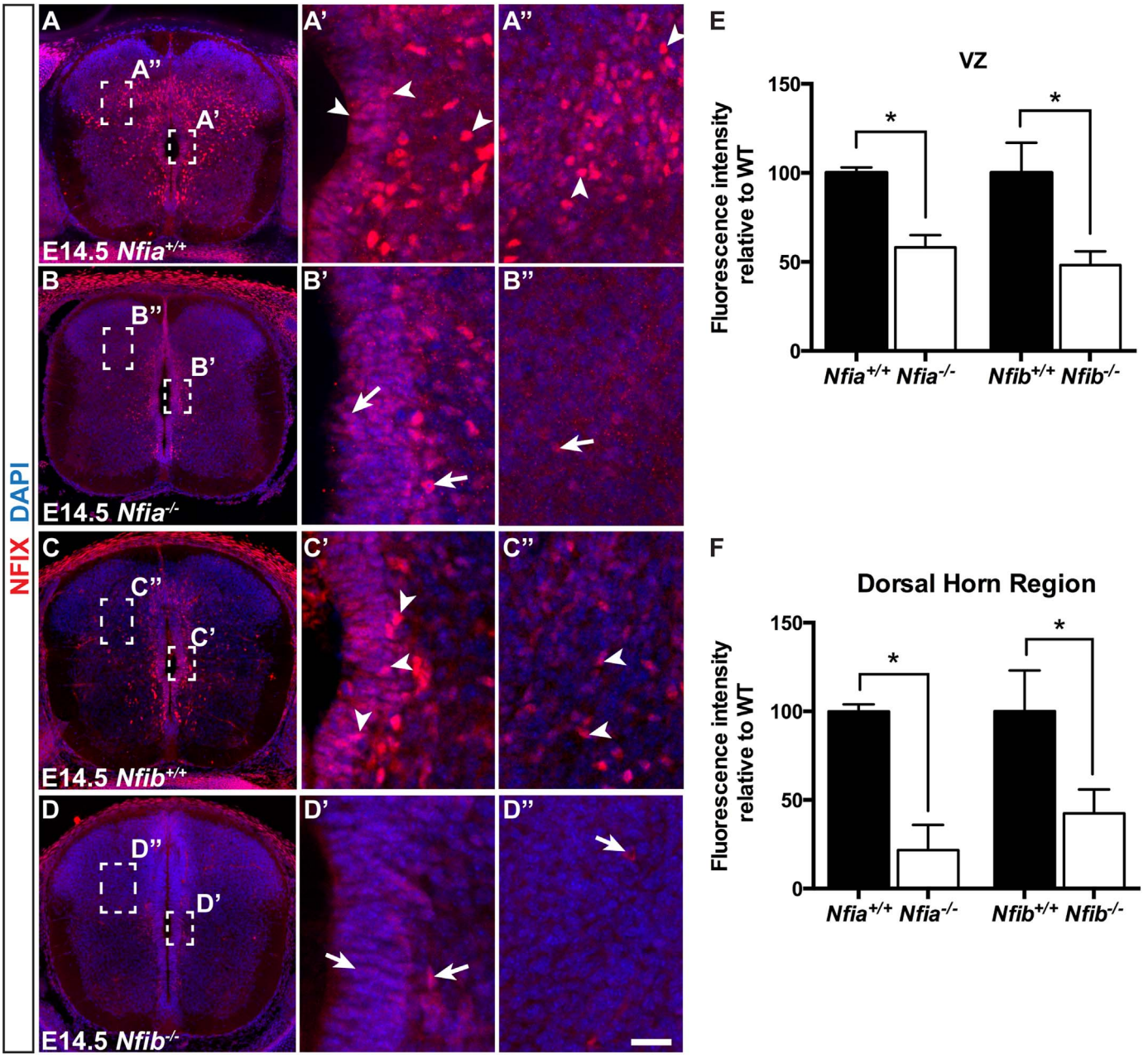

Fig. 7. *Nfia*$^{-/-}$ and *Nfib*$^{-/-}$ mice display decreased NFIX expression. (A-D) The spinal cords of E14.5 *Nfia*$^{-/-}$ and *Nfib*$^{-/-}$ mice, and their wild-type littermate controls, were transversely sectioned and labelled for NFIX using immunofluorescence labelling. The expression of NFIX was reduced in and around the ventricular zone of the spinal cords of *Nfia*$^{-/-}$ (B′; arrows) and *Nfib*$^{-/-}$ (D′; arrows) mice, as well as the dorsal horn regions (B" and D" respectively; arrows) when compared to the controls (arrowheads in A', A'', C', C''). A decrease in NFIX expression was also detected using fluorescence intensity measurements in both the ventricular zone (E) and dorsal horn regions (F). Statistical analyses were performed using a one-sided unpaired non-parametric Mann-Whitney test (n = 3). * $p = 0.05$. Scale bar in (D"): A-D 200 μm; A′-D" 50 μm.

reporter gene assays further demonstrated that NFIB could transcriptionally activate luciferase expression under the control of a portion of the *Nfix* promoter containing the proximal NFI binding site (Fig. 6C, Supp. Fig. 8B). Consistent with our ChIP-qPCR results, NFIA was not able to drive *Nfix*-promoter driven transcriptional activity, although NFIA was able to activate the transcription of the luciferase gene under the control of a different promoter, namely that of the inscuteable gene (Supp. Fig. 8C). Moreover, neither NFIA nor NFIB promoted transcriptional activity driven by a portion of the *Nfix* promoter containing the upstream NFI binding site (data not shown). Collectively, these data suggest that NFIB can directly activate *Nfix*-promoter driven transcriptional activity by binding proximally to the *Nfix* TSS.

3.1.5. NFIX expression is reduced in the spinal cord of Nfib-deficient mice

If *Nfix* were a target of NFIB-mediated transcriptional activity, then we would hypothesise that, as an upstream factor, NFIB expression would be unchanged within *Nfix*$^{-/-}$mice. Conversely, we would posit that NFIX expression would be reduced within the spinal cord of *Nfib*$^{-/-}$ mice. To address these hypotheses, we first assessed protein expression levels in our different knockout strains. As expected, the expression of NFIB within *Nfix*$^{-/-}$mice at E15.5 was comparable to that observed in the controls, as was that of NFIA (Supp. Fig. 9). Next, NFIX protein levels were examined within spinal cord sections from *Nfib*$^{-/-}$ mice. Critically, in line with our *in vitro* data, there was a prominent reduction in the expression of NFIX in *Nfib*$^{-/-}$ mice compared to the

control animals in both the VZ and dorsal horn regions at E14.5 (Fig. 7C-F). Expression of NFIX within the spinal cord was also reduced in E18.5 *Nfib*$^{-/-}$ mice (Supp. Fig. 10). Although we did not find evidence for NFIA binding and regulating the *Nfix* promoter (Fig. 6B, C), we observed a similar phenotype in *Nfia*$^{-/-}$ mice at E14.5, with a reduction in NFIX expression observed in both the VZ and dorsal horn regions in comparison with the wild-type littermates (Fig. 7A, B, E, F). These results suggest an indirect role for NFIA in the regulation of *Nfix* transcription. For example, NFIA may bind distal enhancers not detected in the original ChIP-seq dataset (Mateo et al., 2015) or might regulate *Nfix* expression indirectly. We also identified a putative NFI binding site within the *Nfib* promoter using the same ChIP-seq dataset, suggestive of a mechanism whereby NFIA regulates *Nfib*. However, we saw no change in NFIB protein expression levels within the spinal cord of *Nfia*$^{-/-}$ mice, indicating that *Nfib* is unlikely to be a direct transcriptional target of NFIA (Supp. Fig. 11A-C). In conclusion, we demonstrate that *Nfix* expression is dependent on NFIB-mediated transcriptional regulation, highlighting the importance of the NFI family in regulating gliogenesis within the embryonic spinal cord and revealing that NFIX is part of the downstream transcriptional program through which NFIA and NFIB promote gliogenesis from VZ progenitor cells.

4. Discussion

NFIA and NFIB have previously been identified as critical factors that initiate the gliogenic switch within the embryonic spinal cord (Deneen et al., 2006). The contribution of a third NFI family member, NFIX, to this process was unknown. In this study we identify NFIX as an important component in the development of the embryonic spinal cord, with abnormalities in terminal glial differentiation providing a key insight into the regulation of the astrogliogenic pathway. Additionally, we also identify an interaction between NFI family members along this cell fate pathway by demonstrating the NFIB-mediated activation of *Nfix* expression. This hierarchical organisation of NFI protein expression and function during spinal cord gliogenesis exposes a novel auto-regulatory mechanism working within this family of transcription factors.

Despite the importance of the NFI family for CNS development, the regulatory factors upstream of the *Nfi* genes are poorly defined. Previously, studies have pointed to PAX6 being one factor that could potentially regulate *Nfi* gene expression, as its expression within the dorsal forebrain precedes that of both NFIA and NFIB (Plachez et al., 2008; Walther and Gruss, 1991). Moreover, differential gene expression analysis performed on *Pax6*-deficient mice revealed reduced expression of both *Nfia* and *Nfib* (Holm et al., 2007). However, a recent study demonstrated that *Nfia* and *Nfib* are unlikely to be targets for PAX6-mediated transcriptional control, at least within the embryonic neocortex (Bunt et al., 2015). As such, the transcriptional control of the *Nfi* family remains unclear. Our study points to NFIB as being a key factor in coordinating the timely expression of *Nfix* within the spinal cord. The regulation of *Nfix* by NFIB may also underlie the relatively subtle deficits in terminal astrocytic differentiation observed here, as NFIB itself also likely regulates astrocytic gene expression (Wilczynska et al., 2009). The auto-regulation of transcription factor family gene expression is a recurring theme within nervous system development, and is exhibited for example, by the basic-helix-loop-helix proteins (Akagi et al., 2004), which activate their own transcription during retinal development. The highly overlapping pattern of NFIA, NFIB and NFIX expression in other parts of the developing mouse brain, such as the neocortex (Plachez et al., 2008) and cerebellum (Fraser et al., 2016; Piper et al., 2011; Wang et al., 2007, 2004) suggest that this auto-regulatory function may also operate in these regions too. Interestingly, a recent study that mapped the expression of NFIA, NFIB and NFIX within the adult mouse forebrain revealed that each NFI family member had partially overlapping expression patterns, suggesting that the auto-regulation of NFI expression could also occur within the mature brain (Chen et al., 2017).

This study also provides new insights into our understanding of the transcriptional program controlling the terminal aspects of spinal cord gliogenesis. At this point, the exact targets of NFIX that drive this late-stage astrocyte-specific differentiation remain unknown. Given previous reports, it is likely that NFIX regulates *Gfap* expression (Brun et al., 2009; Singh et al., 2011b). NFIX has also been previously shown to regulate the expression of other astrocytic genes *in vitro*, including the later expressed secreted protein acidic and rich in cysteine-like protein 1 (*SPARCL1*), brain fatty-acid binding protein (*FABP7*), α1-antichymotrypsin (*SERPINA3*) and chitinase 3 like1 (*CHI3L1* or *YKL-40*) (Brun et al., 2009; Gopalan et al., 2006; Piper et al., 2011; Singh et al., 2011a; Wilczynska et al., 2009). To gain further insights into how NFIX controls this cell-fate pathway, methods such as ChIP-seq or RNA-seq could be utilised to determine putative DNA-binding sites or misregulated genes in *Nfix*$^{-/-}$ tissue, respectively. These approaches would provide novel indications as to the downstream targets of NFIX during terminal astrocyte differentiation within the spinal cord.

Interestingly, the ability of NFIs to act as chromatin binding factors may point to them having a broader role in gene regulation outside of the direct binding to promoter or enhancer regions of their direct target genes. An emerging hypothesis has proposed that NFIs modulate chromatin accessibility as epigenetic modifiers (Denny et al., 2016; M. Fane et al., 2017; M.E. Fane et al., 2017b; Pjanic et al., 2013) by binding both the chromatin itself (Pankiewicz et al., 2005), and chromatin modifying proteins (Dusserre and Mermod, 1992; Muller and Mermod, 2000). Here, we analysed the role of NFIX in regulating terminal astrocyte differentiation. However, the ability of NFI proteins to interact with chromatin, or to regulate the expression of chromatin-modifying factors, might help explain the capacity of NFI proteins to govern multiple aspects of neural stem cell fate in other regions, including neuronal differentiation in the dorsal telencephalon and cerebellum (Harris et al., 2016; Piper et al., 2011) and the postnatal production of oligodendrocytes (Zhou et al., 2015).

In conclusion, these findings support previous work indicating that NFI transcription factors act sequentially during astrocytic development, with NFIX acting after NFIA and NFIB during this process (Wilczynska et al., 2009). Crucially our findings reveal additional complexity to this program of NFI-mediated astrocytic gene expression, as we demonstrate that NFIB can bind to the *Nfix* promoter region, driving transcriptional activity. Collectively, these findings provide significant insights into how astrogliogenesis within the embryonic spinal cord is mediated by this family of transcription factors, which may have broad implications in our understanding of diseases or injuries characterised by aberrations in astrocyte production.

Acknowledgements

Imaging work was performed in the Queensland Brain Institute's Advanced Microscopy Facility. This work was funded by an Australian Research Council (ARC) Discovery Project to MP (DP160100368), a National Health and Medical Research Council (NHMRC) Project Grant to LJR (1100443) and by NYSTEM grants (grant numbers C030133 and C026429) to RMG. MP was supported by an ARC Future Fellowship (FT120100170). LJR was supported by an NHMRC Principal Research Fellowship. EM, LH and JWCL were supported by Australian Postgraduate Research Awards.

Conflict of interest

Authors report no conflict of interest

Appendix A. Supplementary material

Supplementary data associated with this article can be found in the online version at http://dx.doi.org/10.1016/j.ydbio.2017.10.019.

References

Akagi, T., Inoue, T., Miyoshi, G., Bessho, Y., Takahashi, M., Lee, J.E., Guillemot, F., Kageyama, R., 2004. Requirement of multiple basic helix-loop-helix genes for retinal neuronal subtype specification. J. Biol. Chem. 279, 28492–28498.

Barry, G., Piper, M., Lindwall, C., Moldrich, R., Mason, S., Little, E., Sarkar, A., Tole, S., Gronostajski, R.M., Richards, L.J., 2008. Specific glial populations regulate hippocampal morphogenesis. J. Neurosci. 28, 12328–12340.

Briscoe, J., Pierani, A., Jessell, T.M., Ericson, J., 2000. A homeodomain protein code specifies progenitor cell identity and neuronal fate in the ventral neural tube. Cell 101, 435–445.

Briscoe, J., Sussel, L., Serup, P., Hartigan-O'Connor, D., Jessell, T.M., Rubenstein, J.L., Ericson, J., 1999. Homeobox gene Nkx2.2 and specification of neuronal identity by graded Sonic hedgehog signalling. Nature 398, 622–627.

Brun, M., Coles, J.E., Monckton, E.A., Glubrecht, D.D., Bisgrove, D., Godbout, R., 2009. Nuclear factor I regulates brain fatty acid-binding protein and glial fibrillary acidic protein gene expression in malignant glioma cell lines. J. Mol. Biol. 391, 282–300.

Bunt, J., Lim, J.W., Zhao, L., Mason, S., Richards, L.J., 2015. PAX6 does not regulate Nfia and Nfib expression during neocortical development. Sci. Rep. 5, 10668.

Butler, S.J., Bronner, M.E., 2015. From classical to current: analyzing peripheral nervous system and spinal cord lineage and fate. Dev. Biol. 398, 135–146.

Cahoy, J.D., Emery, B., Kaushal, A., Foo, L.C., Zamanian, J.L., Christopherson, K.S., Xing, Y., Lubischer, J.L., Krieg, P.A., Krupenko, S.A., Thompson, W.J., Barres, B.A., 2008. A transcriptome database for astrocytes, neurons, and oligodendrocytes: a new resource for understanding brain development and function. J. Neurosci. 28, 264–278.

Campbell, C.E., Piper, M., Plachez, C., Yeh, Y.T., Baizer, J.S., Osinski, J.M., Litwack, E.D., Richards, L.J., Gronostajski, R.M., 2008. The transcription factor Nfix is essential for normal brain development. BMC Dev. Biol. 8, 52.

Caspary, T., Anderson, K.V., 2003. Patterning cell types in the dorsal spinal cord: what the mouse mutants say. Nat. Rev. Neurosci. 4, 289–297.

Chaudhry, A.Z., Lyons, G.E., Gronostajski, R.M., 1997. Expression patterns of the four nuclear factor I genes during mouse embryogenesis indicate a potential role in development. Dev. Dyn. 208, 313–325.

Chen, K.-S., Harris, L., Lim, J.W.C., Harvey, T.J., Piper, M., Gronostajski, R.M., Richards, L.J., Bunt, J., 2017. Differential neuronal and glial expression of Nuclear factor I proteins in the cerebral cortex of adult mice. J. Comp. Neurol. 525, 2465–2483.

das Neves, L., Duchala, C.S., Tolentino-Silva, F., Haxhiu, M.A., Colmenares, C., Macklin, W.B., Campbell, C.E., Butz, K.G., Gronostajski, R.M., 1999. Disruption of the murine nuclear factor I-A gene (Nfia) results in perinatal lethality, hydrocephalus, and agenesis of the corpus callosum. Proc. Natl. Acad. Sci. USA 96, 11946–11951.

Deneen, B., Ho, R., Lukaszewicz, A., Hochstim, C.J., Gronostajski, R.M., Anderson, D.J., 2006. The transcription factor NFIA controls the onset of gliogenesis in the developing spinal cord. Neuron 52, 953–968.

Denny, S.K., Yang, D., Chuang, C.H., Brady, J.J., Lim, J.S., Gruner, B.M., Chiou, S.H., Schep, A.N., Baral, J., Hamard, C., Antoine, M., Wislez, M., Kong, C.S., Connolly, A.J., Park, K.S., Sage, J., Greenleaf, W.J., Winslow, M.M., 2016. Nfib promotes metastasis through a widespread increase in chromatin accessibility. Cell 166, 328–342.

Dusserre, Y., Mermod, N., 1992. Purified cofactors and histone H1 mediate transcriptional regulation by CTF/NF-I. Mol. Cell Biol. 12, 5228–5237.

Ellis, P., Fagan, B.M., Magness, S.T., Hutton, S., Taranova, O., Hayashi, S., McMahon, A., Rao, M., Pevny, L., 2004. SOX2, a persistent marker for multipotential neural stem cells derived from embryonic stem cells, the embryo or the adult. Dev. Neurosci. 26, 148–165.

Ericson, J., Rashbass, P., Schedl, A., Brenner-Morton, S., Kawakami, A., van Heyningen, V., Jessell, T.M., Briscoe, J., 1997. Pax6 controls progenitor cell identity and neuronal fate in response to graded Shh signaling. Cell 90, 169–180.

Fallier-Becker, P., Vollmer, J.P., Bauer, H.C., Noell, S., Wolburg, H., Mack, A.F., 2014. Onset of aquaporin-4 expression in the developing mouse brain. Int. J. Dev. Neurosci. 36, 81–89.

Fane, M., Harris, L., Smith, A.G., Piper, M., 2017a. Nuclear factor one transcription factors as epigenetic regulators in cancer. Int. J. Cancer 140, 2634–2641.

Fane, M.E., Chhabra, Y., Hollingsworth, D.E., Simmons, J.L., Spoerri, L., Oh, T.G., Chauhan, J., Chin, T., Harris, L., Harvey, T.J., Muscat, G.E., Goding, C.R., Sturm, R.A., Haass, N.K., Boyle, G.M., Piper, M., Smith, A.G., 2017b. NFIB mediates BRN2 driven melanoma cell migration and invasion Through regulation of EZH2 and MITF. EBioMedicine 16, 63–75.

Fazi, F., Rosa, A., Fatica, A., Gelmetti, V., De Marchis, M.L., Nervi, C., Bozzoni, I., 2005. A minicircuitry comprised of microRNA-223 and transcription factors NFI-A and C/EBPalpha regulates human granulopoiesis. Cell 123, 819–831.

Fraser, J., Essebier, A., Gronostajski, R.M., Boden, M., Wainwright, B.J., Harvey, T.J., Piper, M., 2016. Cell-type-specific expression of NFIX in the developing and adult cerebellum. Brain Struct. Funct. 222, 2251–2270.

Glasgow, S.M., Laug, D., Brawley, V.S., Zhang, Z., Corder, A., Yin, Z., Wong, S.T., Li, X.N., Foster, A.E., Ahmed, N., Deneen, B., 2013. The miR-223/nuclear factor I-A axis regulates glial precursor proliferation and tumorigenesis in the CNS. J. Neurosci. 33, 13560–13568.

Gopalan, S.M., Wilczynska, K.M., Konik, B.S., Bryan, L., Kordula, T., 2006. Nuclear factor-1-X regulates astrocyte-specific expression of the alpha1-antichymotrypsin and glial fibrillary acidic protein genes. J. Biol. Chem. 281, 13126–13133.

Harris, L., Dixon, C., Cato, K., Heng, Y.H., Kurniawan, N.D., Ullmann, J.F., Janke, A.L., Gronostajski, R.M., Richards, L.J., Burne, T.H., Piper, M., 2013. Heterozygosity for nuclear factor one x affects hippocampal-dependent behaviour in mice. PLoS One 8, e65478.

Harris, L., Genovesi, L.A., Gronostajski, R.M., Wainwright, B.J., Piper, M., 2015. Nuclear factor one transcription factors: divergent functions in developmental versus adult stem cell populations. Dev. Dyn. 244, 227–238.

Harris, L., Zalucki, O., Gobius, I., McDonald, H., Osinki, J., Harvey, T.J., Essebier, A., Vidovic, D., Gladwyn-Ng, I., Burne, T.H., Heng, J.I., Richards, L.J., Gronostajski, R.M., Piper, M., 2016. Transcriptional regulation of intermediate progenitor cell generation during hippocampal development. Development 143, 4620–4630.

Harris, L., Zalucki, O., Oishi, S., Burne, T.H., Jhaveri, D.J., Piper, M., 2017. A morphology independent approach for identifying dividing adult neural stem cells in the mouse hippocampus. Dev. Dyn.. http://dx.doi.org/10.1002/dvdy.24545.

Heng, Y.H., McLeay, R.C., Harvey, T.J., Smith, A.G., Barry, G., Cato, K., Plachez, C., Little, E., Mason, S., Dixon, C., Gronostajski, R.M., Bailey, T.L., Richards, L.J., Piper, M., 2014. NFIX regulates neural progenitor cell differentiation during hippocampal morphogenesis. Cereb. Cortex 24, 261–279.

Hochstim, C., Deneen, B., Lukaszewicz, A., Zhou, Q., Anderson, D.J., 2008. Identification of positionally distinct astrocyte subtypes whose identities are specified by a homeodomain code. Cell 133, 510–522.

Holm, P.C., Mader, M.T., Haubst, N., Wizenmann, A., Sigvardsson, M., Gotz, M., 2007. Loss- and gain-of-function analyses reveal targets of Pax6 in the developing mouse telencephalon. Mol. Cell Neurosci. 34, 99–119.

Kang, P., Lee, H.K., Glasgow, S.M., Finley, M., Donti, T., Gaber, Z.B., Graham, B.H., Foster, A.E., Novitch, B.G., Gronostajski, R.M., Deneen, B., 2012. Sox9 and NFIA coordinate a transcriptional regulatory cascade during the initiation of gliogenesis. Neuron 74, 79–94.

Mason, S., Piper, M., Gronostajski, R.M., Richards, L.J., 2009. Nuclear factor one transcription factors in CNS development. Mol. Neurobiol. 39, 10–23.

Mateo, J.L., van den Berg, D.L., Haeussler, M., Drechsel, D., Gaber, Z.B., Castro, D.S., Robson, P., Crawford, G.E., Flicek, P., Ettwiller, L., Wittbrodt, J., Guillemot, F., Martynoga, B., 2015. Characterization of the neural stem cell gene regulatory network identifies OLIG2 as a multifunctional regulator of self-renewal. Genome Res. 25, 41–56.

Matsuda, T., Cepko, C.L., 2004. Electroporation and RNA interference in the rodent retina in vivo and in vitro. Proc. Natl. Acad. Sci. USA 101, 16–22.

Muller, K., Mermod, N., 2000. The histone-interacting domain of nuclear factor I activates simian virus 40 DNA replication in vivo. J. Biol. Chem. 275, 1645–1650.

Pankiewicz, R., Karlen, Y., Imhof, M.O., Mermod, N., 2005. Reversal of the silencing of tetracycline-controlled genes requires the coordinate action of distinctly acting transcription factors. J. Gene Med. 7, 117–132.

Piper, M., Harris, L., Barry, G., Heng, Y.H., Plachez, C., Gronostajski, R.M., Richards, L.J., 2011. Nuclear factor one X regulates the development of multiple cellular populations in the postnatal cerebellum. J. Comp. Neurol. 519, 3532–3548.

Piper, M., Plachez, C., Zalucki, O., Fothergill, T., Goudreau, G., Erzurumlu, R., Gu, C., Richards, L.J., 2009. Neuropilin 1-Sema signaling regulates crossing of cingulate pioneering axons during development of the corpus callosum. Cereb. Cortex 19 (Suppl 1), 11–21, (i).

Pjanic, M., Schmid, C.D., Gaussin, A., Ambrosini, G., Adamcik, J., Pjanic, P., Plasari, G., Kerschgens, J., Dietler, G., Bucher, P., Mermod, N., 2013. Nuclear Factor I genomic binding associates with chromatin boundaries. BMC Genom. 14, 99.

Plachez, C., Lindwall, C., Sunn, N., Piper, M., Moldrich, R.X., Campbell, C.E., Osinski, J.M., Gronostajski, R.M., Richards, L.J., 2008. Nuclear factor I gene expression in the developing forebrain. J. Comp. Neurol. 508, 385–401.

Rolando, C., Erni, A., Grison, A., Beattie, R., Engler, A., Gokhale, P.J., Milo, M., Wegleiter, T., Jessberger, S., Taylor, V., 2016. Multipotency of adult hippocampal NSCs in vivo is restricted by Drosha/NFIB. Cell Stem Cell 19, 653–662.

Rowitch, D.H., 2004. Glial specification in the vertebrate neural tube. Nat. Rev. Neurosci. 5, 409–419.

Shibata, T., Yamada, K., Watanabe, M., Ikenaka, K., Wada, K., Tanaka, K., Inoue, Y., 1997. Glutamate transporter GLAST is expressed in the radial glia-astrocyte lineage of developing mouse spinal cord. J. Neurosci. 17, 9212–9219.

Singh, S.K., Bhardwaj, R., Wilczynska, K.M., Dumur, C.I., Kordula, T., 2011a. A complex of nuclear factor I-X3 and STAT3 regulates astrocyte and glioma migration through the secreted glycoprotein YKL-40. J. Biol. Chem. 286, 39893–39903.

Singh, S.K., Wilczynska, K.M., Grzybowski, A., Yester, J., Osrah, B., Bryan, L., Wright, S., Griswold-Prenner, I., Kordula, T., 2011b. The unique transcriptional activation domain of nuclear factor-I-X3 is critical to specifically induce marker gene expression in astrocytes. J. Biol. Chem. 286, 7315–7326.

Steele-Perkins, G., Plachez, C., Butz, K.G., Yang, G., Bachurski, C.J., Kinsman, S.L., Litwack, E.D., Richards, L.J., Gronostajski, R.M., 2005. The transcription factor gene Nfib is essential for both lung maturation and brain development. Mol. Cell Biol. 25, 685–698.

Stolt, C.C., Wegner, M., 2010. SoxE function in vertebrate nervous system development. Int. J. Biochem. Cell Biol. 42, 437–440.

Tsuyama, J., Bunt, J., Richards, L.J., Iwanari, H., Mochizuki, Y., Hamakubo, T., Shimazaki, T., Okano, H., 2015. MicroRNA-153 regulates the acquisition of gliogenic competence by neural stem cells. Stem Cell Rep. 5, 365–377.

Walther, C., Gruss, P., 1991. Pax-6, a murine paired box gene, is expressed in the developing CNS. Development 113, 1435–1449.

Wang, W., Mullikin-Kilpatrick, D., Crandall, J.E., Gronostajski, R.M., Litwack, E.D., Kilpatrick, D.L., 2007. Nuclear factor I coordinates multiple phases of cerebellar granule cell development via regulation of cell adhesion molecules. J. Neurosci. 27, 6115–6127.

Wang, W., Stock, R.E., Gronostajski, R.M., Wong, Y.W., Schachner, M., Kilpatrick, D.L., 2004. A role for nuclear factor I in the intrinsic control of cerebellar granule neuron gene expression. J. Biol. Chem. 279, 53491–53497.

Wilczynska, K.M., Singh, S.K., Adams, B., Bryan, L., Rao, R.R., Valerie, K., Wright, S., Griswold-Prenner, I., Kordula, T., 2009. Nuclear factor I isoforms regulate gene expression during the differentiation of human neural progenitors to astrocytes. Stem Cells 27, 1173–1181.

Wong, Y.W., Schulze, C., Streichert, T., Gronostajski, R.M., Schachner, M., Tilling, T., 2007. Gene expression analysis of nuclear factor I-A deficient mice indicates delayed brain maturation. Genome Biol. 8, R72.
Yokoo, H., Nobusawa, S., Takebayashi, H., Ikenaka, K., Isoda, K., Kamiya, M., Sasaki, A., Hirato, J., Nakazato, Y., 2004. Anti-human Olig2 antibody as a useful immunohistochemical marker of normal oligodendrocytes and gliomas. Am. J. Pathol. 164, 1717–1725.
Yuan, J.S., Reed, A., Chen, F., Stewart, C.N., Jr., 2006. Statistical analysis of real-time PCR data. BMC Bioinform. 7, 85.
Zhou, B., Osinski, J.M., Mateo, J.L., Martynoga, B., Sim, F.J., Campbell, C.E., Guillemot, F., Piper, M., Gronostajski, R.M., 2015. Loss of NFIX transcription factor biases postnatal neural stem/progenitor cells toward oligodendrogenesis. Stem Cells Dev. 24, 2114–2126.